The Transcription Factor *Zfp503* Promotes the D1 MSN Identity and Represses the D2 MSN Identity

Zhuangzhi Zhang (zz_zhang@fudan.edu.cn)
Fudan University https://orcid.org/0000-0002-9860-6689

Zicong Shang
Fudan University

Lin Yang
Fudan University

Ziwu Wang
Fudan University

Yu Tian
Fudan University

Yanjing Gao
Fudan University

Zihao Su
Fudan University

Rongliang Guo
Fudan University

Weiwei Li
Fudan University

Guoping Liu
Fudan University

Xiaosu Li
Fudan University

Zhengang Yang
Institutes of Brain Science, Fudan University https://orcid.org/0000-0003-2447-6540

Zhenmeiyu Li
Fudan University

Article

Keywords: Zfp503, striatum, fate switch, LGE, medium-sized spiny neurons

Posted Date: May 4th, 2022

DOI: https://doi.org/10.21203/rs.3.rs-1561923/v1

Abstract

The striatum is primarily composed of two types of medium spiny neurons (MSNs) expressing either D1- or D2-type dopamine receptors. However, the fate determination of these two types of neurons is not fully understood. Here, we found that D1 MSNs undergo fate switching to D2 MSNs in the absence of *Zfp503*. Furthermore, scRNA-seq revealed that the transcription factor *Zfp503* affects the differentiation of these progenitor cells in the lateral ganglionic eminence (LGE). More importantly, we found that the transcription factors *Sp8/9*, which are required for the differentiation of D2 MSNs, are repressed by *Zfp503*. Finally, sustained *Zfp503* expression in LGE progenitor cells promoted the D1 MSN identity and repressed the D2 MSN identity. Overall, *Zfp503* promotes the D1 MSN identity and represses the D2 MSN identity by regulating *Sp8/9* expression during striatal MSN development.

Introduction

The striatum, the major component of the basal ganglia, consists of the caudate and putamen in humans. The majority of striatal neurons are medium-sized spiny neurons (MSNs), which can be further divided into two cell types: one cell type that expresses the dopamine receptor DRD1 (D1 MSNs) and another cell type that expresses the dopamine receptor DRD2 (D2 MSNs). D1 MSNs directly project to the substantia nigra pars reticulata to form the direct pathway, whereas D2 MSNs give rise to the indirect pathway, which projects to the external part of the globus pallidus [1, 2, 3]. Dysfunction of the striatum is closely associated with multiple neuropsychiatric diseases, including Huntington's disease (HD), Parkinson's disease (PD), schizophrenia and obsessive-compulsive disorder/attention deficit hyperactivity disorder [2, 4, 5]. The diversity of striatal function is critically dependent on the normal development of MSNs at the embryonic stage. Previous studies have shown that the lateral ganglionic eminence (LGE), the primordium of the striatum, contains two distinct regions: a dorsal region (dLGE) and a ventral region (vLGE). The dLGE generates most interneurons of the olfactory bulb. In contrast, the vLGE mainly gives rise to striatal MSNs [6, 7, 8, 9, 10, 11]. Initially, the transcription factors (TFs) *Gsx1/2*, *Ascl1*, *Dlx1/2* and *Meis2* control the differentiation of progenitors into immature MSNs [9, 12, 13, 14, 15, 16, 17, 18, 19]. Although D1 MSNs and D2 MSNs share many properties, they specifically express different molecules to fate acquisition [20, 21, 22, 23]. Our previous studies showed that the TFs *Sp8/9* and *Six3* are specifically required for the differentiation of most D2 MSNs [24, 25, 26]. Although many studies have reported that some TFs control the differentiation of subpopulation D1 MSNs [27, 28, 29, 30, 31], the TFs that specifically guid the differentiation of most D1 MSNs still need to be further explored. To date, two studies have indicated that the transcription factor *Zfp503* is required for the differentiation of D1 MSNs [32, 33]. However, the mechanism involved in these processes is still largely unknown.

Here we investigated the role of *Zfp503* in the development of striatal MSNs. *Zfp503* is specifically expressed in most striatal MSNs at later stages of striatal development. We used *Sp9-Cre* and *Dlx2-Cre* to knock out *Zfp503* expression in the ganglionic eminences (GEs) and found switching of D1 MSNs to D2 MSNs in *Zfp503* conditional knockout (*Zfp503*-CKO) mice. Furthermore, our scRNA-seq revealed that D1

MSNs mature earlier (at E14.5) than D2 MSNs. At the cell population level, we found that progenitor cells and D2 MSNs were increased but D1 MSNs were significantly decreased in the LGE of *Zfp503*-CKO mice. Finally, we found that the TFs *Sp8/9* were significantly increased in the LGE of *Zfp503*-CKO mice. *Zfp503* gain of function experiments showed promotion of the D1 MSN identity and repression of the D2 MSN identity. Taken together, our findings suggest that the TF *Zfp503* promotes D1 MSN cell identity and represses D2 MSN cell identity by regulating *Sp8/9* expression during striatal development.

Results

D1 MSNs Are Converted into D2 MSNs in Zfp503-CKO Mice.

Previously, we and others reported that *Zfp503* is highly expressed in the LGE [19, 34, 35], but the expression pattern of *Zfp503* during striatal development is not fully understood. Thus, we performed double immunostaining of ZFP503 with the pan-striatal MSN marker BCL11B at E14.5 and E18.5 (Figs. 1A–A'). Our results showed that approximately 90% of BCL11B positive cells are ZFP503/BCL11B double-positive cells in the subventricular zone (SVZ), but the percentage was decreased to 70% in the mantle zone (MZ) at E14.5 (Fig. 1B). Interestingly, nearly all BCL11B-positive cells were colabelled with ZFP503 in the SVZ/MZ at E18.5 (Fig. 1B). These results indicated that *Zfp503* expression gradually increases in the LGE during striatal MSN development.

To examine the role of *Zfp503* in regulating the fate of MSNs, we used two Cre lines (*Sp9-Cre* and *Dlx2-Cre*) to delete the expression of *Zfp503* in the basal ganglia. The phenotype of the *Zfp503* mutant mice was analyzed at E18.5. We found that there was no significant difference in BCL11B expression between control mice and *Zfp503*-CKO mice (Fig. 1C). These results were further confirmed by our RNA-seq data (Fig. 1D) and were consistent with previous research [33]. *Drd1* and *Tac1*, which are specifically expressed in D1 MSNs were dramatically decreased in the striatum of *Zfp503*-CKO mice compared to controls. In contrast, *Drd2* and *Penk*, which are specifically expressed in D2 MSNs, were markedly increased in *Zfp503*-CKO mice (Fig. 1C). Next, we analysed the phenotype of the *Zfp503*-CKO mice at the transcriptional level. RNA-seq of the entire LGE was performed at E18.5. Again, our results showed that D1 MSN marker genes (*Drd1*, *Tac1*, *Isl1*, *Sox8* and *Pdyn*) were significantly decreased. In contrast, D2 MSN marker genes (*Drd2*, *Penk*, *Six3*, *Grik3* and *Gucy1a3*) were significantly increased (Fig. 1D). Taken together, our results indicated that striatal D1 MSNs are converted into D2 MSNs in the absence of *Zfp503*.

Maturation of D1 MSNs Occurs Earlier Than That of D2 MSNs

To investigate the mechanism by which *Zfp503* control fate switching between D1 and D2 MSNs, two scRNA-seq experiments were performed to analyze LGE progenitors undergoing fate switching (Fig. 2A). LGE samples from E14.5 wild-type (WT, n = 4) and *Zfp503*-DCKO (*Dlx2-Cre; Zfp503$^{F/F}$*, n = 3) mice were dissected, dissociated into single-cell suspensions, and sequenced using the 10X genomics platform.

After removing outlier cells that had a high percentage of ribosomal or mitochondrial genes, 14001 cells in the WT samples and 12225 cells in the *Zfp503*-DCKO samples were used for analysis, with an average of 2107 genes detected per cell (Fig. 2B). Our initial clustering analysis revealed 16 (C0-C15) major cell populations with distinct gene expression patterns (Fig. 2B **and Table 1)**. We used marker genes to define the identities of the 16 clusters more precisely, which resulted in 8 discrete populations: RGs, APs, BPs, IPs, Pre-MSNs, imm-D1 MSNs, D1 MSNs and D2 MSNs (Fig. 2C **and Table 1)**. According to analysis of marker genes **(Table 1)**, we determined the identity of the remaining cell clusters: C7: striatal interneurons (*Lhx6*, *Lhx8*, *Sst* and *Npy*); C9: cortical projection neurons (*Neurod6*, *Tbr1* and *Cux2*); C10: intercalated cells (*Zic1* and *Resp18*); C11: ependymal cells (*S100a11*, *Anxa2* and *Cryab*); C12: endothelial cells (*Cdh5* and *Cd34*); C13: blood cells (*Alas2*); C14: microglial cells (*Bcl2a1b*, *P2ry12* and *Trem2*); and C15: oligodendrocyte cells (*Olig1/2* and *Sox10*).

Next, we systematically characterized the gene features of the D1 and D2 MSNs. To data, the generation sequence of D1 and D2 MSNs during striatal development is not fully understood. Interestingly, we found very low expression levels of *Drd1* and *Drd2* suggesting that the D1 and D2 MSNs were not fully matured at E14.5 (Fig. 2D). However, D1 MSN marker genes (*Tac1* and *Ebf1*) were highly expressed. In contrast, D2 MSN marker genes (*Penk* and *Adora2a*) were weakly expressed (Fig. 2D). Furthermore, the pan-striatal MSN markers (*Rarb*, *Rxrg* and *Foxp1*) were highly expressed in D1 MSNs but not in D2 MSNs (Fig. 2D). In addition, it was previously reported that *Isl1* is highly expressed in immature D1 MSNs [30, 31]. We found that *Pou3f1* and *Aldh1a3* are specifically expressed in immature D1 MSNs. These results indicated that *Pou3f1* and *Aldh1a3* represent new markers for immature D1 MSNs. Taken together, our results suggested that D1 MSN maturation is faster than D2 MSN maturation.

Blocking Differentiation of LGE Progenitors in Zfp503-DCKO Mice

Next, we explored the mechanism underlying fate switching between D1 MSNs and D2 MSNs in *Zfp503*-DCKO (*Dlx2-Cre; Zfp503*$^{F/F}$) mice. Thus, we focused our further analysis on the major cell types in the LGE at E14.5 (Fig. 3A). The radial glia cells (RGs) that expressed *Aldh1l1* and *Aldoc* were not significantly altered between *Zfp503*-DCKO mice and WT mice (Figs. 3B-C **and L)**. *Sox2* is highly expressed in the progenitors of the LGE and downregulated in immature neurons. Surprisingly, our results showed that *Sox2* expression was upregulated in most cell types, especially in immature MSNs in *Zfp503*-DCKO mice (Figs. 3D **and L)**. Recent studies reported that *Ascl1* and *Vax1* are highly expressed in basal progenitors (BPs) [11, 36, 37], and a study showed that *Gadd45g* is a direct downstream target of *Ascl1* [38]. These genes were increased in the *Zfp503*-DCKO mice (Figs. 3E-G **and L)**. We also found that the proliferating cells expressing *Ki67* (*Mki67*) and *Top2a* were increased in the *Zfp503*-DCKO mice compared to the WT mice (Figs. 3H-I **and L)**. Finally, our results showed that *Dlx2* and its direct downstream target *Gad2* were increased in MSNs (Figs. 3J-L). Taken together, these findings indicated that the differentiation of progenitors is blocked in *Zfp503*-DCKO mice.

Zfp503 Promotes the D1 MSN Identity and Represses the D2 MSNs Identity

To further confirm our results regarding D1 and D2 MSN identity at the cell population level, we begin to analyze D1 and D2 MSN clusters in our scRNA-seq data. Previous work and our studies showed that *Pou3f1*, *Isl1* and *Zfhx3* are highly expressed in immature D1 MSNs [27, 30, 31]. We found that the expression of these genes in the immature D1 MSN cluster was not significantly changed between WT mice and *Zfp503*-DCKO mice (Figs. 4A-C **and O)**. However, *Ebf1*, *Ikzf1*, *Tac1*, *Rarb* and *Foxp2*, which were highly expressed in D1 MSNs were significantly reduced in the D1 MSN cluster of *Zfp503*-DCKO mice compared to wild-type mice (Figs. 4D-H **and O)**. Our previous studies showed that theTFs *Sp9* and *Six3* are required for the differentiation of D2 MSNs [24, 25, 26]. In the absence of *Zfp503*, these genes were upregulated in D2 MSNs (Figs. 4I-J). Furthermore, *Tle4* and *Gucy1a3* trend to be expressed in D2 MSNs, and our results showed that these genes were upregulated in D2 MSNs and immature D1 MSNs in *Zfp503*-DCKO mice (Figs. 4K-L). In addition, the specific D2 MSN markers *Penk* and *Adora2a* were upregulated in *Zfp503*-DCKO mice compared to WT mice (Figs. 4M-O). Again, our findings indicated that D1 MSNs undergo fate switching into D2 MSNs at the cell population level in *Zfp503*-DCKO mice.

Zfp503 **Represses the D2 MSN Identity by Regulating** Sp8/9 **Expression**

To gain insights into the mechanism by which *Zfp503* regulates the fate switching of striatal MSNs, we performed immunostaining at E16.5 and E18.5. The TF *Sox2* is mainly expressed in radial glial cells located in the LGE VZ and downregulated in striatal MSNs (Fig. 5A). Our previous studies demonstrated that the TFs *Sp8/9* and *Six3* are required for the differentiation of D2 MSNs. Furthermore, the TFs *Sp8/9* directly regulate *Six3* expression by binding its promoter [24, 25, 26]. Surprisingly, we found that *Sox2* was significantly upregulated in the whole striatum at E16.5 and E18.5 in *Zfp503*-DCKO mice compared to controls (Figs. 5A-D and 6A-D). Considering that striatal MSNs express relatively mature markers, such as *Drd1* and *Penk* (Figs. 1C-D), we speculate that the striatal MSNs is not well differentiated due to blockade of differentiation at the progenitor stage. Moreover, our results showed that the TFs *Sp8/9* were dramatically increased in the striatum at E16.5 and E18.5 in the *Zfp503*-CKO mice compared to controls (Figs. 5E-L and 6E-L). Interestingly, *Sp8* expression was significantly increased at E16.5 (Figs. 5I-L) and E14.5 (data not shown) in both Cre lines, but the expression of *Sp8* was not altered at E18.5 in the *Dlx2-Cre* line (Figs. 6I-L). The *Dlx2-Cre* deleted *Zfp503* expression in LGE radial glial cells and the *Sp9-Cre* deleted *Zfp503* expression in progenitors located in the LGE SVZ. Therefore, we speculated that *Zfp503* promotes cell cycle exit of radial glial cells, which leads to *Sp8* expression showing the different phenotypes at different time points. In addition, *Six3*, a direct downstream target of *Sp8/9* was significantly increased in *Zfp503*-CKO mice at E16.5 and E18.5 (Figs. 5M-P and 6M-P). Taken together, these findings suggested that *Zfp503* represses the D2 MSN identity by controlling the expression of *Sp8/9*.

Overexpression of Zfp503 **Promote the D1 MSN Identity and Suppress the D2 MSN Identity**

In addition to investigating the effects of *Zfp503* loss-of-function, we also explored the effects of *Zfp503* gain-of-function in striatal MSNs. First, we generated a *Zfp503* overexpression allele (*Zfp503*-OE). A CAG promoter followed by a *Zfp503* CDS and three HA-tag sequences was inserted into the *Rosa-26* site with

the CRISPR/Cas9 strategy (Fig. 7A). Then, we crossed *Zfp503-OE* mice with *Dlx2-Cre* mice to obtain *Zfp503* overexpressing mice (*Dlx2-Cre; Zfp503-OE*). *Dlx2-Cre; Zfp503-OE* embryos showed robust Ha-tag signals in *Dlx2*-expressing regions along the dorso-ventral (DV) axis, including the septum, striatum, and cortex interneuron (Fig. 7B). To study the function of *Zfp503* in regulating the cell identity of striatal MSNs, we used in situ hybridization to detect the expression of D1 MSN and D2 MSN markers. Consistent with our expectations, the expression of *Isl1*, *Tac1* and *Ebf1* was increased in the *Zfp503* overexpressing mice (Figs. 7C-E). In contrast, TFs *Sp9* and *Six3*, which control the differentiation of D2 MSNs were reduced in *Zfp503* overexpressing mice compared to control mice (Figs. 7F-G). In addition, the RNA-seq data showed that the D1 MSN identity was enhanced and the D2 MSN identity was compromised in the *Dlx5/6-Cre*; *Zfp503*-OE mice compared to the control mice (Figs. 7H). Overall, our findings suggested that *Zfp503* promotes the D1 MSN identity and represses the D2 MSN identity.

Discussion

The generation of striatal D1 versus D2 MSNs is controlled by different TFs. In this study, we found that the TF *Zfp503* is intensely expressed in MSNs during striatal development. The absence of *Zfp503* resulted in fate switching of D1 MSNs into D2 MSNs. Single-cell RNA-seq and histochemical analyses revealed that *Zfp503* promotes the D1 MSN identity and represses the D2 MSN identity. Mechanistically, the upregulation of the TFs *Sp8/9* is the key factor leading to the switching of D1 MSNs to the D2 MSNs in *Zfp503*-CKO mice. Overall, we speculate that TF *Zfp503* controls the fate of D1 MSNs by repressing *Sp8/9* expression during striatal development.

D1 MSNs and D2 MSNs Are Generated in Distinct Domains in the LGE

Understanding the mechanisms underlying neuronal fate acquisition is a major challenge in developmental neurobiology, because there are many distinct regions and different progenitors in the mammalian telencephalon, particularly in the subpallium [6, 8, 11, 39, 40]. More recent evidence has shown that TF *Zfp503* expression is enriched in the ventral parts of the vLGE [33], while the TF *Six3* expression preferentially present in the dorsal parts of the vLGE at an early stage [24]. Furthermore, the differentiation of D1 MSNs and D2 MSNs is completely blocked in *Zfp503*-CKO and *Six3*-CKO mice, respectively [24, 32]. These results support that D1 MSNs are generated from the ventral part of the vLGE, in contrast to D2 MSNs which are derived from the dorsal part of the vLGE.

Retinoic acid (RA) has been implicated as an extrinsic signal regulating the differentiation of distinct cell types, including specific neuronal subtypes [41, 42, 43, 44, 45]. Indeed, the mechanism through which RA signaling regulates limb development has been explored [45, 46, 47]. RA is derived from vitamin A through a two-step enzymatic process, employing retinol dehydrogenase (*Rdh10*) for the oxidation of retinol to retinaldehyde, and the retinaldehyde dehydrogenases *Aldh1a1*, *Aldh1a2*, and *Aldh1a3* for the oxidation of retinaldehyde to RA, which then functions as a ligand for nuclear RA receptors [42]. LGE progenitors begin

to express the *Aldh1a3*, but not *Aldh1a1* and *Aldh1a2* around E12.5 and are located in the ventral vLGE [42, 48]. During striatal development, *Aldh1a3* is predominantly expressed in LGE (striatal primordium) progenitors and is nearly absent in adjacent structures of the medial ganglionic eminence and cerebral cortex [41, 48]. Its expression is regulated by *Gsx2* and *Meis2* [49]. In fact, the expression of the *Aldh1a3* is located in the ventral vLGE [42, 49, 50, 51]. The roles of RA in the LGE have been investigated, including promoting striatal neurogenesis and neuronal differentiation [43, 48, 52, 53, 54]. The absence of *Aldh1a3* leads to abnormal differentiation of striatal MSNs [42]. Interestingly, RA can promote the expression of *Zfp503* in the LGE at the early stage of striatal development [52]. These studies support that RA can induce *Zfp503* expression in ventral vLGE progenitors at an early stage. In this work, we found that *Zfp503* promotes the D1 MSN identity and represses the D2 MSN identity. Therefore, we speculate that the progenitors located in the ventral vLGE trend to give rise to D1 MSNs. In contrast, the progenitors located in the dorsal vLGE trend to generate D2 MSNs.

Foxp2 **Expression Was Inhibited by** Six3 **in the D2 MSN Lineage.**

The Forkhead box P2 (FOXP2) has been identified as a gene related to neurodevelopmental disorders, and it was also the first gene to be associated with vocal functions in songbirds and rodents [55, 56]. Indeed, mutations in the FOXP2 gene have been identified in patients with a severe speech and language disorders [57]. Naturally, *Foxp2* is enriched in the striatum and controls the differentiation of striatal MSNs [55, 57, 58, 59, 60]. The mechanisms, however, of regulating *Foxp2* expression in the striatum are largely unknown. More recent evidence supports that *Foxp2* is highly expressed in D1 MSNs and weakly expressed in the D2 MSNs [58, 61]. In this study, we found that the expression of *Foxp2* was significantly reduced in *Zfp503*-DCKO mice (Fig. 4H). Interestingly, the expression of *Six3* was present in the whole striatum (Figs. 6M-O). *Six3* is known as a key factor for the generation of D2 MSNs [24, 26]. Thus, we speculated that *Six3* represses the expression of *Foxp2* in D2 MSNs. Actually, in our recent works and unpublished data, we found that *Foxp2* expression is upregulated in *Six3* mutant mice and downregulated in *Six3* overexpressing mice [24, 26]. Therefore, our findings suggested that *Foxp2* expression is closely regulated by *Six3* in D2 MSNs.

Overall, our findings have demonstrated that *Zfp503* is critical for the fate acquisition of D1 versus D2 MSNs during striatal development. *Zfp503* appears to repress the expression of the TF *Sp8/9* in precursor cells to control the fate of D1 MSNs. The results of this work will deepen our understanding of fate determination in striatal MSNs and open up new opportunities for translational investigations of degenerative diseases, such as PD and HD.

Declarations

COMPETING INTERESTS

We declare that there is no conflict of interest.

DATA AVAILABILITY STATEMENT

The data that support the findings of this study are available from the corresponding author upon reasonable request.

AUTHOR CONTRIBUTIONS

Z.S., L.Y. and Z.W. performed all experiments and analyzed data. Y.T., Y.G., Z.S., R.G., W.L., G.L., X.L. and W.Z. helped to conduct experiments and analyze the data. Z.Z. and Z.L. designed the experiments and analyzed the results. Z.Z., and Z.Y. wrote the manuscript and revised the manuscript.

FUNDING

This study was supported by grants from National Key Research and Development Program of China (2018YFA0108000, 2021ZD0202300), National Natural Science Foundation of China (NSFC 31820103006, NSFC 32070971 and NSFC32100768), and supported by Shanghai Municipal Science and Technology Major Project (No.2018SHZDZX01), ZJ Lab, and Shanghai Center for Brain Science and Brain-Inspired Technology.

ACKNOWLEDGMENTS

We are grateful to Kenneth Campbell at University of Cincinnati College of Medicine for the *Dlx5/6*-CIE mice.

References

1. Gerfen CR, Engber TM, Mahan LC, Susel Z, Chase TN, Monsma FJ, Jr*., et al.* D1 and D2 dopamine receptor-regulated gene expression of striatonigral and striatopallidal neurons. *Science* 1990, **250**(4986)**:** 1429-1432.

2. Gerfen CR, Surmeier DJ. Modulation of striatal projection systems by dopamine. *Annu Rev Neurosci* 2011, **34:** 441-466.

3. Kawaguchi Y, Wilson CJ, Augood SJ, Emson PC. Striatal interneurones: chemical, physiological and morphological characterization. *Trends Neurosci* 1995, **18**(12)**:** 527-535.

4. DeLong MR. Primate models of movement disorders of basal ganglia origin. *Trends Neurosci* 1990, **13**(7)**:** 281-285.

5. Wichmann T, DeLong MR. Functional and pathophysiological models of the basal ganglia. *Curr Opin Neurobiol* 1996, **6**(6)**:** 751-758.

6. Stenman J, Toresson H, Campbell K. Identification of two distinct progenitor populations in the lateral ganglionic eminence: implications for striatal and olfactory bulb neurogenesis. *J Neurosci* 2003,

23(1)**:** 167-174.

7. Waclaw RR, Allen ZJ, 2nd, Bell SM, Erdelyi F, Szabo G, Potter SS*, et al.* The zinc finger transcription factor Sp8 regulates the generation and diversity of olfactory bulb interneurons. *Neuron* 2006, **49**(4)**:** 503-516.

8. Yun K, Potter S, Rubenstein JL. Gsh2 and Pax6 play complementary roles in dorsoventral patterning of the mammalian telencephalon. *Development* 2001, **128**(2)**:** 193-205.

9. Anderson SA, Qiu M, Bulfone A, Eisenstat DD, Meneses J, Pedersen R*, et al.* Mutations of the homeobox genes Dlx-1 and Dlx-2 disrupt the striatal subventricular zone and differentiation of late born striatal neurons. *Neuron* 1997, **19**(1)**:** 27-37.

10. Olsson M, Campbell K, Wictorin K, Bjorklund A. Projection neurons in fetal striatal transplants are predominantly derived from the lateral ganglionic eminence. *Neuroscience* 1995, **69**(4)**:** 1169-1182.

11. Wen Y, Su Z, Wang Z, Yang L, Liu G, Shang Z*, et al.* Transcription Factor VAX1 Regulates the Regional Specification of the Subpallium Through Repressing Gsx2. *Molecular Neurobiology* 2021, **58**(8)**:** 3729-3744.

12. Waclaw RR, Wang B, Pei Z, Ehrman LA, Campbell K. Distinct temporal requirements for the homeobox gene Gsx2 in specifying striatal and olfactory bulb neuronal fates. *Neuron* 2009, **63**(4)**:** 451-465.

13. Wang B, Waclaw RR, Allen ZJ, 2nd, Guillemot F, Campbell K. Ascl1 is a required downstream effector of Gsx gene function in the embryonic mouse telencephalon. *Neural Dev* 2009, **4:** 5.

14. Pei Z, Wang B, Chen G, Nagao M, Nakafuku M, Campbell K. Homeobox genes Gsx1 and Gsx2 differentially regulate telencephalic progenitor maturation. *Proceedings of the National Academy of Sciences* 2011, **108**(4)**:** 1675-1680.

15. Wang B, Long JE, Flandin P, Pla R, Waclaw RR, Campbell K*, et al.* Loss of Gsx1 and Gsx2 function rescues distinct phenotypes in Dlx1/2 mutants. *Journal of Comparative Neurology* 2013, **521**(7)**:** 1561-1584.

16. Chapman H, Riesenberg A, Ehrman LA, Kohli V, Nardini D, Nakafuku M*, et al.* Gsx transcription factors control neuronal versus glial specification in ventricular zone progenitors of the mouse lateral ganglionic eminence. *Dev Biol* 2018, **442**(1)**:** 115-126.

17. Yun K, Garel S, Fischman S, Rubenstein JL. Patterning of the lateral ganglionic eminence by the Gsh1 and Gsh2 homeobox genes regulates striatal and olfactory bulb histogenesis and the growth of axons through the basal ganglia. *J Comp Neurol* 2003, **461**(2)**:** 151-165.

18. Long JE, Swan C, Liang WS, Cobos I, Potter GB, Rubenstein JL. Dlx1&2 and Mash1 transcription factors control striatal patterning and differentiation through parallel and overlapping pathways. *J Comp Neurol* 2009, **512**(4)**:** 556-572.

19. Su Z, Wang Z, Lindtner S, Yang L, Shang Z, Tian Y*, et al.* Dlx1/2-dependent expression of Meis2 promotes neuronal fate determination in the mammalian striatum. *Development* 2022, **149**(4).

20. Lobo MK, Karsten SL, Gray M, Geschwind DH, Yang XW. FACS-array profiling of striatal projection neuron subtypes in juvenile and adult mouse brains. *Nat Neurosci* 2006, **9**(3)**:** 443-452.

21. Gokce O, Stanley GM, Treutlein B, Neff NF, Camp JG, Malenka RC*, et al.* Cellular Taxonomy of the Mouse Striatum as Revealed by Single-Cell RNA-Seq. *Cell Rep* 2016, **16**(4)**:** 1126-1137.

22. Stanley G, Gokce O, Malenka RC, Südhof TC, Quake SR. Continuous and Discrete Neuron Types of the Adult Murine Striatum. *Neuron* 2019.

23. Puighermanal E, Castell L, Esteve-Codina A, Melser S, Kaganovsky K, Zussy C*, et al.* Functional and molecular heterogeneity of D2R neurons along dorsal ventral axis in the striatum. *Nat Commun* 2020, **11**(1)**:** 1957.

24. Xu Z, Liang Q, Song X, Zhang Z, Lindtner S, Li Z*, et al.* Sp8 and Sp9 coordinately promote D2-type medium spiny neuron production by activating Six3 expression. *Development* 2018.

25. Zhang Q, Zhang Y, Wang C, Xu Z, Liang Q, An L*, et al.* The Zinc Finger Transcription Factor Sp9 Is Required for the Development of Striatopallidal Projection Neurons. *Cell Rep* 2016, **16**(5)**:** 1431-1444.

26. Song X, Chen H, Shang Z, Du H, Li Z, Wen Y*, et al.* Homeobox Gene Six3 is Required for the Differentiation of D2-Type Medium Spiny Neurons. *Neurosci Bull* 2021, **37**(7)**:** 985-998.

27. Zhang Z, Wei S, Du H, Su Z, Wen Y, Shang Z*, et al.* Zfhx3 is required for the differentiation of late born D1-type medium spiny neurons. *Exp Neurol* 2019**:** 113055.

28. Garel S, Marin F, Grosschedl R, Charnay P. Ebf1 controls early cell differentiation in the embryonic striatum. *Development* 1999, **126**(23)**:** 5285-5294.

29. Lobo MK, Yeh C, Yang XW. Pivotal role of early B-cell factor 1 in development of striatonigral medium spiny neurons in the matrix compartment. *J Neurosci Res* 2008, **86**(10)**:** 2134-2146.

30. Ehrman LA, Mu X, Waclaw RR, Yoshida Y, Vorhees CV, Klein WH*, et al.* The LIM homeobox gene Isl1 is required for the correct development of the striatonigral pathway in the mouse. *Proc Natl Acad Sci U S A* 2013, **110**(42)**:** E4026-4035.

31. Lu KM, Evans SM, Hirano S, Liu FC. Dual role for Islet-1 in promoting striatonigral and repressing striatopallidal genetic programs to specify striatonigral cell identity. *Proc Natl Acad Sci U S A*

2014, **111**(1)**:** E168-177.

32. Soleilhavoup C, Travaglio M, Patrick K, Garcao P, Boobalan E, Adolfs Y*, et al.* Nolz1 expression is required in dopaminergic axon guidance and striatal innervation. *Nat Commun* 2020, **11**(1)**:** 3111.

33. Chen SY, Lu KM, Ko HA, Huang TH, Hao JH, Yan YT*, et al.* Parcellation of the striatal complex into dorsal and ventral districts. *Proc Natl Acad Sci U S A* 2020.

34. Ko HA, Chen SY, Chen HY, Hao HJ, Liu FC. Cell type-selective expression of the zinc finger-containing gene Nolz-1/Zfp503 in the developing mouse striatum. *Neurosci Lett* 2013, **548:** 44-49.

35. Chang CW, Tsai CW, Wang HF, Tsai HC, Chen HY, Tsai TF*, et al.* Identification of a developmentally regulated striatum-enriched zinc-finger gene, Nolz-1, in the mammalian brain. *Proc Natl Acad Sci U S A* 2004, **101**(8)**:** 2613-2618.

36. Li X, Liu G, Yang L, Li Z, Zhang Z, Xu Z*, et al.* Decoding Cortical Glial Cell Development. *Neurosci Bull* 2021.

37. Bocchi VD, Conforti P, Vezzoli E, Besusso D, Cappadona C, Lischetti T*, et al.* The coding and long noncoding single-cell atlas of the developing human fetal striatum. *Science* 2021, **372**(6542).

38. Huang HS, Kubish GM, Redmond TM, Turner DL, Thompson RC, Murphy GG*, et al.* Direct transcriptional induction of Gadd45gamma by Ascl1 during neuronal differentiation. *Mol Cell Neurosci* 2010, **44**(3)**:** 282-296.

39. Flames N, Pla R, Gelman DM, Rubenstein JL, Puelles L, Marin O. Delineation of multiple subpallial progenitor domains by the combinatorial expression of transcriptional codes. *J Neurosci* 2007, **27**(36)**:** 9682-9695.

40. Corbin JG, Rutlin M, Gaiano N, Fishell G. Combinatorial function of the homeodomain proteins Nkx2.1 and Gsh2 in ventral telencephalic patterning. *Development* 2003, **130**(20)**:** 4895-4906.

41. Toresson H, Mata de Urquiza A, Fagerstrom C, Perlmann T, Campbell K. Retinoids are produced by glia in the lateral ganglionic eminence and regulate striatal neuron differentiation. *Development* 1999, **126**(6)**:** 1317-1326.

42. Chatzi C, Brade T, Duester G. Retinoic acid functions as a key GABAergic differentiation signal in the basal ganglia. *PLoS Biol* 2011, **9**(4)**:** e1000609.

43. Rataj-Baniowska M, Niewiadomska-Cimicka A, Paschaki M, Szyszka-Niagolov M, Carramolino L, Torres M*, et al.* Retinoic Acid Receptor beta Controls Development of Striatonigral Projection Neurons through FGF-Dependent and Meis1-Dependent Mechanisms. *J Neurosci* 2015, **35**(43)**:** 14467-14475.

44. Podleśny-Drabiniok A, Sobska J, de Lera AR, Gołembiowska K, Kamińska K, Dollé P*, et al.* Distinct retinoic acid receptor (RAR) isotypes control differentiation of embryonal carcinoma cells to dopaminergic or striatopallidal medium spiny neurons. *Scientific Reports* 2017, **7**(1).

45. Cunningham TJ, Duester G. Mechanisms of retinoic acid signalling and its roles in organ and limb development. *Nat Rev Mol Cell Biol* 2015, **16**(2)**:** 110-123.

46. Ghyselinck NB, Duester G. Retinoic acid signaling pathways. *Development* 2019, **146**(13).

47. Berenguer M, Duester G. Role of Retinoic Acid Signaling, FGF Signaling and Meis Genes in Control of Limb Development. *Biomolecules* 2021, **11**(1).

48. Molotkova N, Molotkov A, Duester G. Role of retinoic acid during forebrain development begins late when Raldh3 generates retinoic acid in the ventral subventricular zone. *Dev Biol* 2007, **303**(2)**:** 601-610.

49. Waclaw RR, Wang B, Campbell K. The homeobox gene Gsh2 is required for retinoid production in the embryonic mouse telencephalon. *Development* 2004, **131**(16)**:** 4013-4020.

50. Li H, Wagner E, McCaffery P, Smith D, Andreadis A, Drager UC. A retinoic acid synthesizing enzyme in ventral retina and telencephalon of the embryonic mouse. *Mech Dev* 2000, **95**(1-2)**:** 283-289.

51. Smith D, Wagner E, Koul O, McCaffery P, Dräger UC. Retinoic acid synthesis for the developing telencephalon. *Cereb Cortex* 2001, **11**(10)**:** 894-905.

52. Urban N, Martin-Ibanez R, Herranz C, Esgleas M, Crespo E, Pardo M*, et al.* Nolz1 promotes striatal neurogenesis through the regulation of retinoic acid signaling. *Neural Dev* 2010, **5:** 21.

53. Liao WL, Tsai HC, Wang HF, Chang J, Lu KM, Wu HL*, et al.* Modular patterning of structure and function of the striatum by retinoid receptor signaling. *Proc Natl Acad Sci U S A* 2008, **105**(18)**:** 6765-6770.

54. Al Tanoury Z, Gaouar S, Piskunov A, Ye T, Urban S, Jost B*, et al.* Phosphorylation of the retinoic acid receptor RAR 2 is crucial for the neuronal differentiation of mouse embryonic stem cells. *Journal of Cell Science* 2014, **127**(9)**:** 2095-2105.

55. Chiu YC, Li MY, Liu YH, Ding JY, Yu JY, Wang TW. Foxp2 regulates neuronal differentiation and neuronal subtype specification. *Dev Neurobiol* 2014, **74**(7)**:** 723-738.

56. Bacon C, Rappold GA. The distinct and overlapping phenotypic spectra of FOXP1 and FOXP2 in cognitive disorders. *Human genetics* 2012, **131**(11)**:** 1687-1698.

57. Lai CS, Fisher SE, Hurst JA, Vargha-Khadem F, Monaco AP. A forkhead-domain gene is mutated in a severe speech and language disorder. *Nature* 2001, **413**(6855)**:** 519-523.

58. van Rhijn J-R, Fisher SE, Vernes SC, Nadif Kasri N. Foxp2 loss of function increases striatal direct pathway inhibition via increased GABA release. *Brain Structure and Function* 2018.

59. Chen YC, Kuo HY, Bornschein U, Takahashi H, Chen SY, Lu KM*, et al.* Foxp2 controls synaptic wiring of corticostriatal circuits and vocal communication by opposing Mef2c. *Nat Neurosci* 2016, **19**(11)**:** 1513-1522.

60. Fong WL, Kuo HY, Wu HL, Chen SY, Liu FC. Differential and Overlapping Pattern of Foxp1 and Foxp2 Expression in the Striatum of Adult Mouse Brain. *Neuroscience* 2018, **388:** 214-223.

61. Tinterri A, Menardy F, Diana MA, Lokmane L, Keita M, Coulpier F*, et al.* Active intermixing of indirect and direct neurons builds the striatal mosaic. *Nature Communications* 2018, **9**(1).

62. Wei S, Du H, Li Z, Tao G, Xu Z, Song X*, et al.* Transcription factors Sp8 and Sp9 regulate the development of caudal ganglionic eminence-derived cortical interneurons. *J Comp Neurol* 2019.

63. Liu Z, Zhang Z, Lindtner S, Li Z, Xu Z, Wei S*, et al.* Sp9 Regulates Medial Ganglionic Eminence-Derived Cortical Interneuron Development. *Cerebral Cortex* 2018.

64. Yang L, Su Z, Wang Z, Li Z, Shang Z, Du H*, et al.* Transcriptional profiling reveals the transcription factor networks regulating the survival of striatal neurons. *Cell death & disease* 2021, **12**(3)**:** 262-262.

Materials And Methods

Animals

All experiments conducted in this study were in accordance with guidelines from Fudan University, China. *Zfp503*$^{F/+}$ [19], *Sp9-Cre* [25], and *Dlx5/6-CIE* [62] mice have been previously described. *Dlx2-Cre* mice were generated via the CRISPR/Cas9 strategy. IRES elements and *Cre* sequences were knocked into the coding region of exon 3 of *Dlx2*. Genotyping of the *Dlx2-Cre* constitutive knock-in (KI) allele was performed by PCR using the following primers:

F1: 5'- CCTCGGCCTTTCTGGGAAACTAC-3';

R1: 5'- CTTGCAGGTACAGGAGGTAGTCC-3';

R2: 5'- TTGGCACTAAAGGATCCCACGAG-3'. These primers yielded bands of 390 and 501 bp for the WT and knock-in (KI) alleles, respectively. Rosa26-*Zfp503*-OE/+ mice that conditionally overexpressed *Zfp503* were generated by CRISPR/Cas9 techniques (Figure 7A). An expression vector containing CAG-promoter-Flox-LacZ-PolyA STOP-Flox-*Zfp503*-PolyA was knocked into the Rosa26 locus. With this strategy, the *Zfp503*-HA tag fusion protein was continuously expressed in CRE recombinase-positive cells. In cells

after CRE recombination, both the HA tag and the *Zfp503* protein were specifically detected. Genotyping of the *Zfp503*-OE allele was performed by PCR using the following primers:

WT-F3: 5'-CACTTGCTCTCCCAAAGTCGCTC-3';

WT-R3: 5'-ATACTCCGAGGCGGATCACAA-3';

OE-F5: 5'-GCATCTGACTTCTGGCTAATAAAG-3'. These primers yield bands of 453 and 633 bp for the WT and overexpression alleles, respectively. All mice were maintained in a mixed genetic background of C57BL/6J and CD1. The day of vaginal plug detection was considered E0.5, and the day of birth was defined as P0. Both male and female mice were used in all experiments.

Tissue Preparation

Tissue preparation was performed as previously described [63].

Immunohistochemistry

In this study, 6-μm and 12-μm thick frozen sections were used for immunostaining. The sections were washed with 0.05 M Tris buffered saline (TBS) for 10 min,If necessary, the sections were immersed in antigenic repair solutionpH = 6.0and boiled before the Triton step, and cooled naturally to room temperature (RT) incubated in Triton X-100 (0.5% in 0.05 M TBS) for 30 min at RT, and then incubated with blocking solution (10% donkey serum +0.5%; Triton-X-100 in 0.05 M TBS, pH 7.2) for 2 h at RT. The primary antibodies were diluted in 10% donkey serum blocking solution, incubated overnight at 4°C and then rinsed three times with 0.05 M TBS. Secondary antibodies matching the appropriate species were added and incubated for 2-4 h at RT. Fluorescently stained sections were then washed three times with 0.05 M TBS. This was followed by 4',6-diamidino-2-phenylindole (DAPI) (Sigma-Aldrich, 200 ng/ml) staining for 5 min, and the sections were then cover-slipped with Gel/Mount (Biomeda).

In Situ RNA Hybridization

In situ hybridization (ISH) was performed on 20-μm cryosections using digoxigenin riboprobes as previously described [27, 64]. Probes were made from P0 WT mouse brain cDNA amplified by PCR.

RNA-seq

LGE samples of E16.5 *Zfp503*-OE, E18.5 *Zfp503*-CKO and littermate control mice were dissected (n > = 3 for each group). Total RNA was purified with a Mini RNA Isolation Kit (Zymo) followed by library generation according to the manufacturer's protocol (Illumina TruSeq Stranded Total RNA Library Prep Kit with Ribo-Zero Mouse). Fragment size distribution was assessed using a Bioanalyzer 2100. The concentration of the libraries was measured using a Kapa Library Quantification Kit. The purified libraries were sequenced on a HiSeq 4000 platform. Gene expression levels were reported as fragments per

kilobase of exon per million fragments mapped (FPKM) values. Genes with a P value < 0.05 were considered to be differentially expressed.

Tissue Processing for scRNA-seq

Embryonic mouse (E14.5) brains were quickly collected and placed in HBSS. The LGE samples were dissected and incubated in 1 mg/ml papain in HBSS for 20 min at 37 °C. The tissues were gently dissociated into a single-cell suspension by pipetting. Cells were centrifuged and washed twice, filtered through Flowmi Tip 40 μM strainers, and resuspended in HBSS+ 0.04% BSA. Cell viability was assessed by trypan blue exclusion.

sc-RNA-seq and Analysis

The Chromium Droplet-based Sequencing Platform (10X Genomics) was used to generate scRNA-seq libraries, following the manufacturer's instructions (manual document part number: CG00052 Rev C). The cDNA libraries were purified, quantified using an Agilent 2100 Bioanalyzer, and sequenced on an Illumina HiSeq4000. High quality sequences (clean reads) were obtained by removing low quality sequences and joints. The clean reads were then processed with Cell Ranger software to obtain quantitative information on gene expression. Genes expressed in < 3 cells and cells with < 750 detected genes were filtered out. Cells with >10% mitochondrial genes were also filtered out. The global-scaling normalization method "Log Normalize" was applied to the raw read counts generated by 10X Cell Ranger to normalize the gene expression measurements for each cell based on the total expression. The log-transformed normalized single-cell expression values were used for differential expression tests. Potential sources of variation, including technical noise, batch effects, and biological sources of variation such as cell-cycle stage, were removed to improve downstream dimensionality reduction and clustering. We regressed gene expression on the number of detected molecules per cell and the cell-cycle stage score. The scaled z-scored residuals were used for principal component analysis (PCA). Statistically significant principal components determined by a resampling test were kept for uniform manifold approximation and projection (UMAP) analysis. Differentially-expressed genes (DEGs) among clusters were identified by comparing cells in each cluster against all other cells with the likelihood-ratio test. Gene A was defined as a biomarker of cluster X if it was detected in ≥25% cells, and had an adjusted *P-value* < 5%, and fold change ≥2 between cells of cluster X and all other cells. All these analyses were performed in Seurat v3.2 (https://satijalab.org/seurat/).

Image Acquisition and Statistical Analysis

Images for quantitative analyses were acquired using an Olympus VS 120 microscope with a 20X objective. Bright-field images were acquired using an Olympus VS 120 microscope with a 10X objective. Images were merged, cropped and optimized in Adobe Photoshop CC without distorting the original information. Analyses were performed using GraphPad Prism 6.0, Microsoft Excel and the R language. Unpaired two-tailed *t-test* or one-way ANOVA followed by the Tukey–Kramer post-hoc test was used to

determine statistical significance. All quantification results are presented as the mean ± SEM. Differences with *P-values* < 0.05 were considered significant.

For quantification of $BCL11B^+$ and $ZFP503^+$ cells in the striatum at E14.5 and E18.5, four anatomically matched 6-μm thick coronal sections were selected (n = 3 mice per group). We counted $BCL11B^+$ and $ZFP503^+$ cells in the striatum under a 20X objective lens. The striatum was delineated by DAPI staining. The numbers of $BCL11B^+$ and $ZFP503^+$ cells per section for each LGE SVZ were presented as the relative to these in the control group.

For quantification of $SIX3^+$ and $SP9^+$ cells in the striatum of control and *Zfp503*-CKO mice at E16.5 and E18.5, four anatomically matched 12-μm thick coronal sections were selected (n = 4 mice per group). We used the histogram tool in Adobe Photoshop CC to calculate the fluorescence intensity of $SIX3^+$ and $SP9^+$ cells in the striatum. Data were presented in proportion to the control group.

For quantification of $SP8^+$and $SOX2^+$ cells in the striatum of control and *Zfp503*-CKO mice at E16.5 and E18.5, four anatomically matched 12-μm thick coronal sections were selected (n = 3 mice per group). We counted $SP8^+$and $SOX2^+$ cells in the striatum under a 20X objective lens. The striatum was delineated by DAPI staining. The numbers of $SP8^+$and $SOX2^+$ cells per section for each striatum were presented as the relative to these in the control group.

Table 1

Table 1 is not available with this version.

Figures

Figure 1

Fate switching of D1 MSNs into D2 MSNs in *Zfp503*-CKO mice.

(A) ZFP503/BCL11B double-immunostained coronal hemisection at E14.5. **(A')** High magnification images of the boxed region in A. **(B)** Quantification showing that most of the ZFP503-positive cells in the LGE were colabelled with BCL11B at E14.5 and E18.5. **(C)** BCL11B-positive cells, which represent the vast majority of striatal MSNs, were similar between *Zfp503*-CKO mice and control mice. *Drd1* and *Tac1* expression was significantly decreased whereas *Drd2* and *Penk* expression was markedly increased in the LGE at E18.5 in the *Zfp503*-CKO mice compared to the controls. **(D)** RNA sequencing performed at E18.5 on control and *Sp9-Cre; Zfp503*$^{F/F}$ (*Zfp503*-SCKO) striatal tissues revealed that genes implicated in striatal MSN identity were unaffected. In contrast, the subsets of genes associated with the D1 MSN identity were decreased, whereas the subsets of genes associated with the D2 MSN identity were

increased. (Student's t test, ***P <0.001, n = 4, mean ± SEM). Abbreviations: lateral ventricle (LV), mantle zone (MZ), ventricular zone (VZ), subventricular zone (SVZ). Scale bars: 100 μm in A; 100 μm in A'; 200 μm in C.

Figure 2

The maturation of D1 MSNs occurs earlier than that of D2 MSNs

(A) Workflow of scRNA-seq of LEG samples at E14.5. LGE tissues were dissected from embryos and dissociated into single-cell suspensions. Single cells were captured into droplets with the 10x platform. After sequencing, cells were classified by their transcriptomes. **(B)** UMAP showing 16 clusters (C0–C15); the major cell types are annotated in both the wild-type sample and the *Dlx2-Cre; Zfp503* $^{F/F}$ (*Zfp503*-DCKO) sample. **(C)** Violin plot showing cluster annotations, cell type assignments (y-axis) and the expression of 17 marker genes (x-axis). **(D)** Feature plots of the 12 marker genes in 16 different cell types in the wild-type sample. Abbreviations: radial glia cells (RGs); apical progenitors (Aps); basal progenitors (BPs); intermediate progenitors (IPs); premature MSNs (Pre-MSNs); immature D1 MSNs (Imm-D1 MSNs).

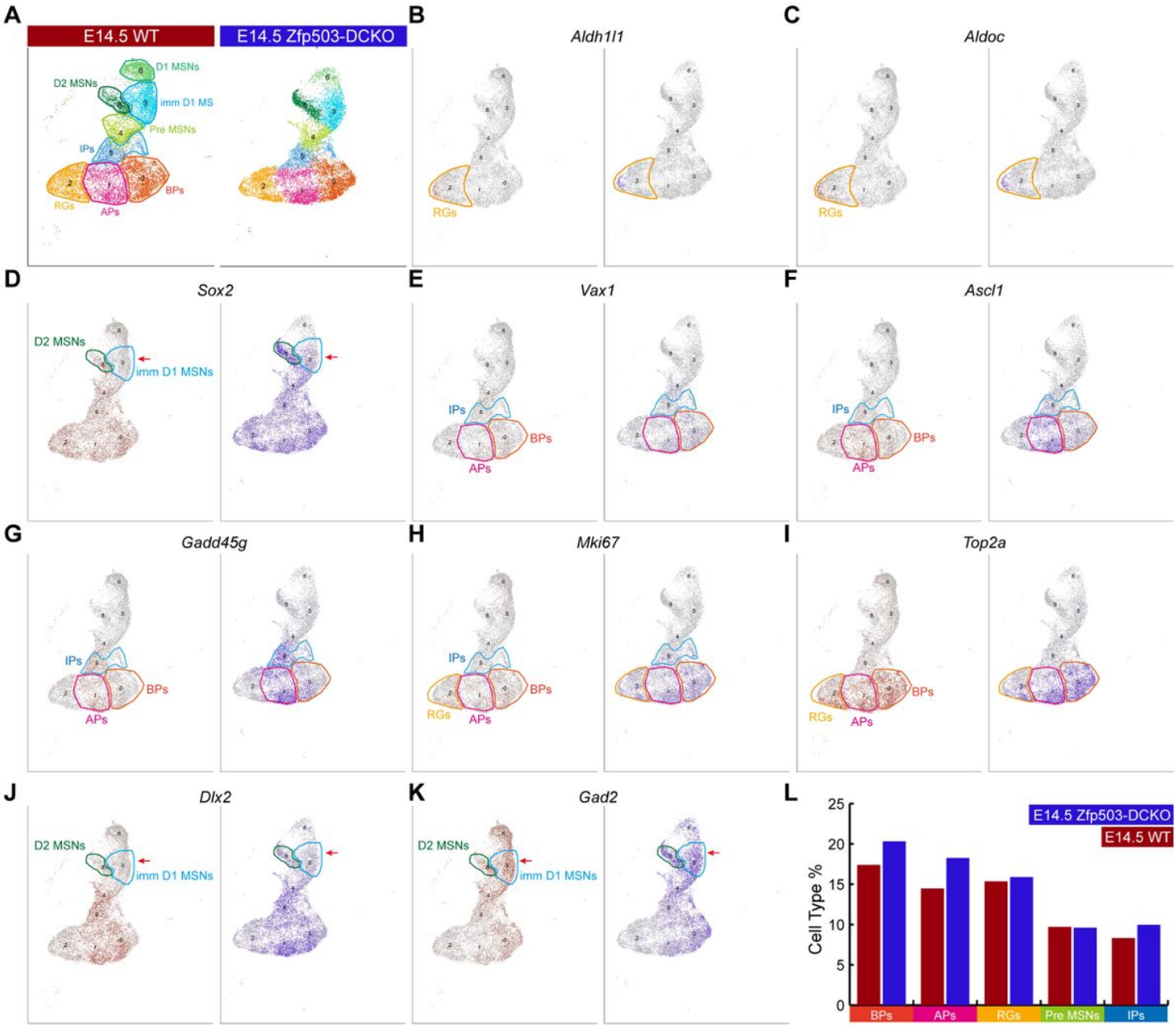

Figure 3

Zfp503 regulates the differentiation of progenitor cells

(A) The major cell populations of the LGE at E14.5. **(B-C)** There were no significant differences in the expression of *Aldh1l1* and *Aldoc* between wild-type (WT) and *Zfp503*-DCKO mice. **(D-K)** The expression of *Sox2*, *Vax1*, *Ascl1*, *Gadd45g*, *Mki67*, *Top2a*, *Dlx2* and *Gad2* was increased in the *Zfp503*-mutant sample compared to the WT sample. **(L)** The percentages of BPs, APs, and IPs were increased but the percentages of RGs and Pre-MSNs were not altered in the *Zfp503*-DCKO sample compared to the WT sample. Abbreviations: radial glia cells (RGs); apical progenitors (Aps); basal progenitors (BPs); intermediate progenitors (IPs); premature MSNs (Pre-MSNs); immature D1 MSNs (Imm D1 MSNs).

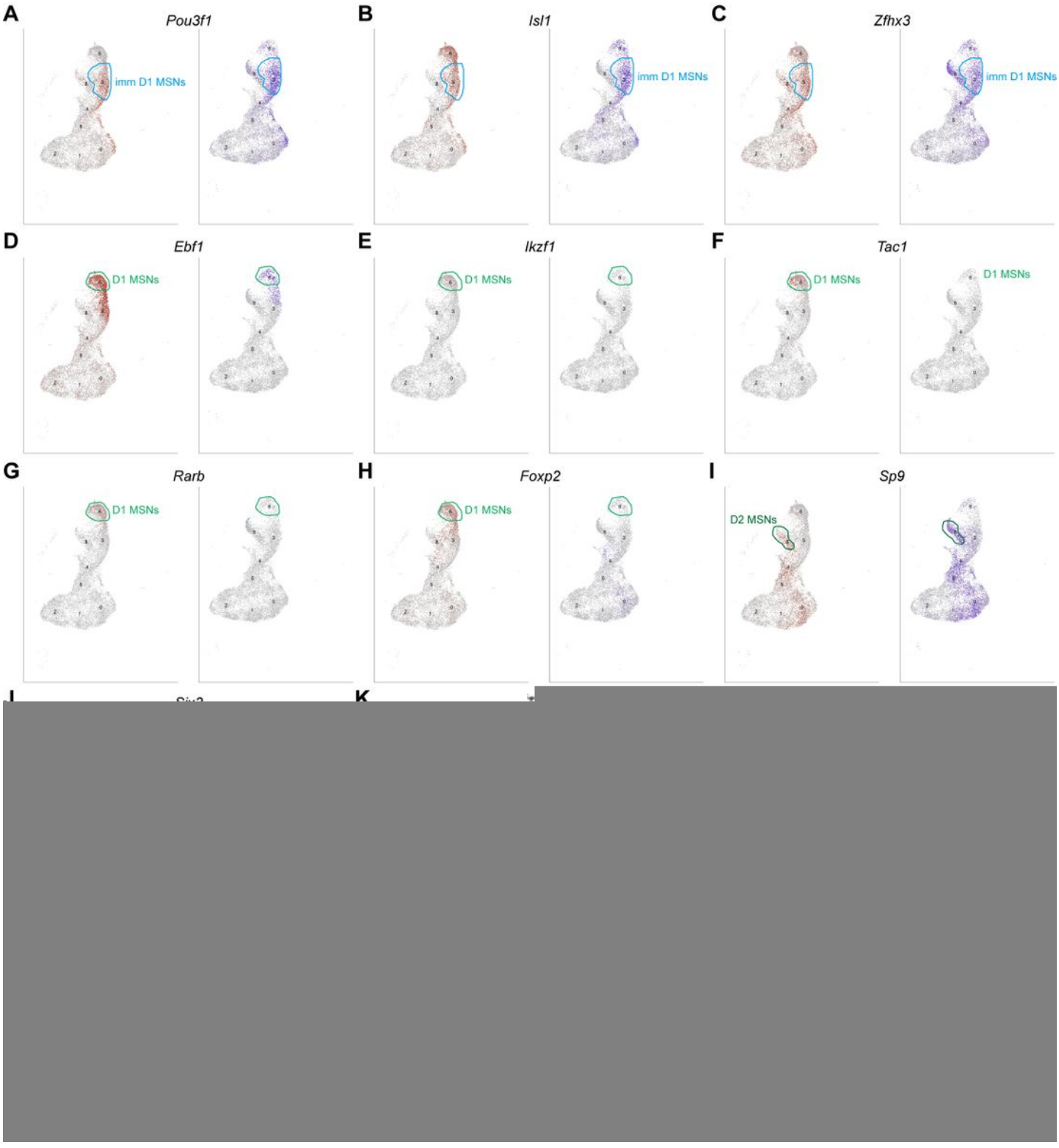

Figure 4

scRNA-seq reveals that *Zfp503* promotes the D1 MSN identity and represses the D2 MSN identity

(A-C) There were no significant changes in the expression of immature D1 MSN markers, including *Pou3f1*, *Isl1* and *Zfhx3,* between *Zfp503*-DCKO mice and WT mice. **(D-H)** The expression of *Ebf1*, *Ikzf1*, *Tac1*, *Rarb* and *Foxp2* was decreased in *Zfp503*-DCKO mice. **(I-N)** The expression of *Sp9*, *Six3*, *Tle4*,

Gucy1a3, *Penk* and *Adora2a* was increased in *Zfp503*-DCKO mice compared to WT mice. **(O)** The cell types percentage in *Zfp503*-DCKO mice and WT mice.

Figure 5

Abnormal expression of precursor marker genes in *Zfp503*-CKO mice at E16.5.

(A-D) The expression of *Sox2* was increased in the entire striatum of *Zfp503*-CKO mice at E16.5. **(E-L)** The transcription factors *Sp8* and *Sp9* were increased in the striatum of *Zfp503*-CKO mice at E16.5. **(M-P)** *Six3* expression was present in the whole striatum in *Zfp503*-CKO mice, but not in control mice. One-way ANOVA followed by the Tukey–Kramer post hoc test, ***P<0.001, n = 3, mean ± SEM. Scale bar: 200 μm in O for A-O.

Figure 6

Abnormal expression of precursor marker genes in the striatum of *Zfp503*-CKO mice at E18.5.

(A-D) The expression of *Sox2* was increased in the entire striatum of *Zfp503* mutants at E18.5. **(E-L)** The transcription factors *Sp8* and *Sp9* were increased in the striatum of *Zfp503*-CKO mice at E18.5. **(M-P)** *Six3* expression was present in the whole striatum in *Zfp503*-CKO mice, but not in control mice. Abbreviations: lateral ventricle (LV). One-way ANOVA followed by Tukey–Kramer post hoc test, ***P<0.001, n = 3, mean ± SEM. Scale bar: 200 μm in O for A-O.

Figure 7

The D1 MSN identity is enhanced and the D2 MSN identity is compromised in *Zfp503*-overexpressing mice

(A) Generation of the *Zfp503* overexpression allele. A CAG promoter followed by a *Zfp503* CDS and three HA tag sequences was inserted into the *Rosa-26* site with the CRISPR/Cas9 strategy. **(B)** HA-tag was expressed in the septum, striatum and cortical interneurons, which is consistent with the increased *Dlx2* expression in the forebrains of *Dlx2-Cre; Zfp503-OE* mice compared to controls. **(C-E)** The expression of *Isl1*, *Tac1* and *Ebf1,* which are specifically expressed in D1 MSNs, was increased in *Dlx2-Cre; Zfp503-OE* mice compared to controls. **(F-G)** The expression of the TFs *Sp9* and *Six3* was reduced in *Dlx2-Cre; Zfp503-OE* mice compared to controls. **(H)** The RNA-seq data showed that the D1 MSN identity was

enhanced and the D2 MSN identity was compromised in *Dlx5/6-Cre*; *Zfp503*-OE mice. N = 3 per group. Scale bar: 100 μm in B for B-G.

Supplementary Files

This is a list of supplementary files associated with this preprint. Click to download.

- ajchecklistCDdisease.pdf